JCTC Journal of Chemical Theory and Computation

Article

pubs.acs.org/JCTC

Simulation of Liquid and Supercritical Hydrogen Sulfide and of Alkali Ions in the Pure and Aqueous Liquid

Esam A. Orabi‡ and Guillaume Lamoureux*

Department of Chemistry and Biochemistry and Centre for Research in Molecular Modeling (CERMM), Concordia University, 7141 Sherbrooke Street West, Montréal, Québec H4B 1R6, Canada

Supporting Information

ABSTRACT: A polarizable model for hydrogen sulfide (H_2S) is optimized based on the experimental properties of the monomer and of the bulk liquid. The model is characterized by rigid SH bonds but flexible HSH angle and the polarizability is based on the Drude oscillator model. Bonded parameters and atomic charges are based on the experimental properties of the gaseous monomer. Atomic Lennard-Jones (LJ) parameters are adjusted based on the density of H_2S around the critical point (in the temperature range 363−393 K and pressure range 8.023−10.013 MPa). The model gives binding energies for H_2S dimers, trimers, and tetramers in good agreement with ab initio MP2(full)/6-311++G(d,p) results. It shows a liquid structure in very good agreement with neutron diffraction data. The model also gives density, self-diffusion coefficient, heat of vaporization, and dielectric constant of liquid hydrogen sulfide at the normal boiling point in good agreement with experimental data. In addition, the model is transferable to high temperature and pressure conditions, as evidenced from simulations up to 542.2 K and 40 MPa. The model is used in combination with the SWM4-NDP water model, with LJ parameters between the S and O atoms adjusted to reproduce the experimental hydration free energy of H_2S. Simulations suggest that, in its first solvation shell, a single H_2O molecule is solvated by 10 H_2S molecules while a single H_2S molecule is solvated by 20.5 H_2O molecules. Pair-specific LJ parameters between alkali ions (Li^+, Na^+, K^+, Rb^+, Cs^+) and the S atom are adjusted to reproduce ab initio binding energies of the ion−H_2S pairs at the CCSD(T) level. Simulations based on these parameters show that alkali ions have higher coordination numbers and lower solvation free energies in liquid H_2S than in liquid water or liquid ammonia. The model is also used to investigate the preferential solvation of the ions in aqueous solutions with a 10% H_2S mole fraction. Results show that the ions are preferentially solvated by water in their first solvation shell but have no significant selectivity to either ligands in their second shells.

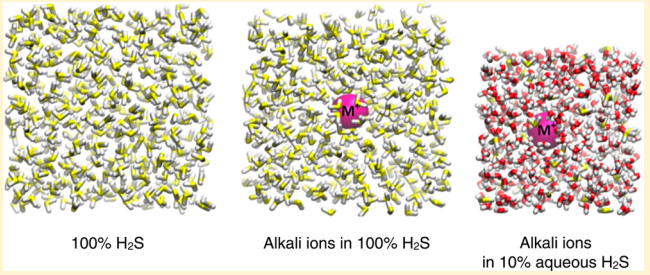

1. INTRODUCTION

Hydrogen sulfide (H_2S) is a colorless gas known to be poisonous, highly corrosive to metals, flammable, and explosive.[1−3] The gas is primarily produced in nature by the bacterial decomposition of organic material, especially under low oxygen concentration, and is listed as a hazardous air pollutant.[3] It is a natural constituent of natural gas and petroleum, and the most common impurity in their hydrocarbon content. H_2S needs thus to be removed from oil and gas, in a process called sweetening.[3] While exposure to concentrated H_2S gas results in symptoms such as irritation, breathing disorder, nausea, diarrhea, rapid heart rate, and headaches, and can cause death,[1−3] H_2S is found to act as a neurotransmitter at very low concentrations.[4]

While H_2S and H_2O share some characteristic properties—both are polar molecules, have a bent molecular geometry, and are amphiprotic—their fluids display significantly different structural, dynamic, and thermodynamic properties. For example, while neutron diffraction experiments show strong hydrogen bonding between water molecules,[5] they indicate that H_2S lacks such hydrogen bonding network.[6] H_2S is also known to display dielectric constant and heat of vaporization lower than those of H_2O. Optimization of potential models for H_2S is thus important to understand the properties of the liquid and to study multicomponent natural-gas mixtures, in order to suggest effective H_2S-separation strategies. Such models would be valuable complements to experiment, given the care that should be taken when working with or in the presence of H_2S (due to its toxicity). In addition, H_2S can be considered a minimal model for the side chains of the amino acids cysteine (Cys) and methionine (Met), and thus reliable potential models for H_2S can be transferred to higher thiol members. Molecular models can be benchmarked using a wealth of experimental data on the pure H_2S fluid: structure,[6] density,[7,8] heat of vaporization,[7,9,10] self-diffusion coefficient,[11] dielectric constant,[12] and heat capacity.[9,13]

The first potential model for liquid H_2S was reported by Jorgensen, as part of a series of intermolecular potential functions for sulfur-containing compounds.[14] This rigid three-

Received: March 19, 2014
Published: June 6, 2014

   dx.doi.org/10.1021/ct5002335 | J. Chem. Theory Comput. 2014, 10, 3221−3235

site model is parameterized to reproduce the heat of vaporization and density of liquid H_2S at the normal boiling point. The model, published before neutron diffraction investigations of the liquid structure,[6] is suggesting significant hydrogen-bonding in liquid H_2S. Forester et al.[15] have parameterized a rigid four-site model, with three atomic sites and a point charge on the bisector of the HSH angle. This model gives heat of vaporization in satisfactory agreement with experiment but underestimates the self-diffusion coefficient of the liquid in the temperature range examined (194−293 K).[15] Kristóf and Liszi[16] have reparameterized the model of Forester et al. to reproduce the density and heat of vaporization over the temperature range 224−353 K of the liquid−vapor coexistence curve of H_2S. Kamath et al.[17] have parameterized a set of four three-site models for H_2S with flexible HSH angles. These four models were adjusted such that the density and vapor pressure in the temperature range 260−370 K are in close agreement with experiments.

Induced polarization is important for the accurate description of liquid water[18] and liquid ammonia,[19,20] which suggests that polarizable molecular models would be superior to pairwise-additive models for H_2S as well (given that polarizability increases in the sequence $H_2O < NH_3 < H_2S$). Most recently, Riahi and Rowley[21] have developed a polarizable model for H_2S composed of four sites (three atomic sites and a point charge at the bisector of the HSH angle) and a Drude oscillator on the sulfur atom. The model was parameterized to reproduce the structural, thermodynamic, and dielectric properties of liquid H_2S at the boiling point, and used to investigate properties of H_2S over the temperature range 212−298 K along the liquid−vapor coexistence curve.

While some of these models[14−17,21] are reported to reproduce experimental properties of H_2S, they have not been validated at temperatures higher than 400 K. Given the difficulty for performing experiments at high temperature and pressure, reliable models at such conditions are desirable.

The solvation structure and solvation thermodynamics of alkali ions in liquid water and liquid ammonia have received considerable attention over the past years.[22−26] In contrast, to the best of our knowledge, no experimental or computational studies of alkali ion solvation in liquid H_2S have ever been reported. Except for the Na^+−H_2S pair,[14] no ab initio studies of alkali ions in H_2S clusters have been reported either. A more systematic ab initio investigation is certainly desirable, given the lack of experimental data. Ab initio calculations can provide information on the geometry and energetics of ion−H_2S complexes, can help explaining the properties of ions in liquid H_2S, and can provide benchmark data for parameterization of potential models. Such models are important to understand the trend in solvation structure and solvation free energy as a function of the ligand hardness (going from the hard H_2O to the less hard NH_3 to the soft H_2S).

Studying the solvation of alkali ions in liquid mixtures is important to understand preferential solvation, which is a determinant factor in ion selectivity in biological systems. In a previous study,[24] we investigated the solvation of alkali ions in liquid ammonia and the ions preferential solvation in ammonia−water mixtures using a Drude polarizable model for ion−NH_3 interactions. Compared to other MM, QM/MM, and QM molecular dynamics (MD) simulation results, the model gave results more consistent with the hard−soft acid−base theory.[24]

In this work, we aim to develop a simple polarizable potential model for liquid H_2S. Compared to the Riahi and Rowley's model,[21] the present model is formed of three atomic sites and a Drude particle on sulfur but has no additional site to describe the electron lone pair. The model is optimized to minimize the error in density of H_2S in the temperature range 363−393 K and pressure range 8.023−10.013 MPa, and to reproduce the hydration free energy of H_2S and the ab initio binding energies of alkali ions-H_2S pairs calculated at the CCSD(T) level. It is then validated on the ab initio binding energies of $(H_2S)_n$ (n = 2−4) clusters calculated at the MP2 level, and on the properties of liquid hydrogen sulfide over a wide range of temperatures and pressures (that covers the liquid and supercritical phases of H_2S). The model is used to investigate the solvation structure and solvation free energy of alkali ions in liquid H_2S. In combination with models for water[18] and for ion−water interactions[26] developed previously, it is also used to investigate the solvation structure of a single H_2S solute in liquid H_2O, the solvation structure of a single H_2O solute in liquid H_2S, and the preferential solvation of alkali ions in aqueous hydrogen sulfide solution at mole fraction $x_{H_2S} = 0.1$.

2. METHODS

2.1. Ab initio Calculations. All ab initio calculations are performed using the Gaussian 09 program.[27] Calculations on H_2S−H_2O pair and $(H_2S)_n$ clusters (n = 1−4) are carried out at the MP2/6-311++G(d,p) level. For $(H_2S)_2$, geometry optimization is also performed at the MP2 level using Dunning's aug-cc-pVXZ basis sets (X = D, T, Q, 5).[28] For M^+−H_2S pairs (M^+ = Li^+, Na^+, and K^+), calculations are performed at the MP2/6-311++G(d,p) level. For the M^+ = Rb^+ and M^+ = Cs^+ complexes, calculations are performed at the MP2 level with the 6-311+G(3df,2p) basis set for H, O, and S atoms, and with the Stuttgart RSC 1997 effective core potentials (ECP) and valence basis sets[29] for Rb and Cs atoms. Diffuse d and f polarization functions are added to the basis sets, with exponents 0.39 and 0.55 for Rb, and 0.29 and 0.44 for Cs.[24] Ab initio calculations on alkali ion−H_2S pairs are also performed using coupled cluster theory with single, double, and perturbative triple excitations (CCSD(T)), with the same basis sets as for the MP2 calculations. All ab initio calculations are done using full-electron representation. Except for the transition state (TS) structures of the H_2S−H_2S and H_2S−H_2O pairs, geometry optimizations are carried out without imposing any symmetry constraints. Frequency calculations are performed on all optimized structures to confirm that they are either energy minima or TSs. The counterpoise (CP) procedure of Boys and Bernardi[30] is used to correct binding energies for basis set superposition error (BSSE).

Potential energy surfaces (PESs) for the H_2S−H_2S and H_2S−H_2O pairs are generated at the MP2/6-311++G(d,p) level by scanning the S···S and S···O distances in optimized structures from 2 to 10 Å. For M^+−H_2S pairs, PESs are generated at the CCSD(T) level with basis sets as described earlier. These PESs are the result of scanning the M^+···S distance from 2 to 10 Å and the M^+···S−Y angle from 0° to 180° (where Y is a point on the bisector of the HSH angle). All surfaces are computed using the geometries of the optimized H_2S and H_2O monomers and are corrected for BSSE.

2.2. Molecular Mechanics Calculations. Molecular mechanics (MM) calculations are performed with the program CHARMM.[31] Polarizable potential models based on classical

Drude oscillators[32] have been reported for H_2O[18] and alkali ions.[26] Following our previous work,[20,24,33−35] a polarizable model for liquid H_2S and alkali ion−H_2S interactions is optimized based on their experimental and ab initio properties.

2.2.1. Potential Energy Function and Parameterization Strategy. In the Drude oscillator model, molecular polarizability is described by attaching a light (0.4 amu), negatively charged "Drude" particle to all non-hydrogen atoms.[32] A harmonic spring with force constant k_D = 1000 kcal/mol·Å^2. is used to tether the Drude particle to the heavy atom.[32] The partial charge q_i of a polarizable atom i is distributed between the Drude particle (q_{Di}) and the atomic core ($q_{ci} = q_i - q_{Di}$) with the Drude particle charge being determined from the atomic polarizability via the relation $\alpha_i = {q_{Di}}^2/k_D$. A displacement d of the Drude particle from the polarizable atom results in a dipole moment $q_{Di}d$. The potential energy function that describes all polarizable systems studied in this work is given by[20,24]

$$U(R) = \sum_{i=1}^{N} \frac{1}{2} k_D |\mathbf{r}_{ci} - \mathbf{r}_{Di}|^2 + \sum_{\text{HSH angles}} k_\theta(\theta - \theta_0)^2 + \sum_{\text{nonbond}} E_{\min,ij}\left[\left(\frac{R_{\min,ij}}{|\mathbf{r}_{ci} - \mathbf{r}_{cj}|}\right)^{12} - 2\left(\frac{R_{\min,ij}}{|\mathbf{r}_{ci} - \mathbf{r}_{cj}|}\right)^{6}\right] + \sum_{\text{nonbond}} \left(\frac{q_{ci}q_{cj}}{|\mathbf{r}_{ci} - \mathbf{r}_{cj}|} + \frac{q_{ci}q_{Dj}}{|\mathbf{r}_{ci} - \mathbf{r}_{Dj}|} + \frac{q_{Di}q_{cj}}{|\mathbf{r}_{Di} - \mathbf{r}_{cj}|} + \frac{q_{Di}q_{Dj}}{|\mathbf{r}_{Di} - \mathbf{r}_{Dj}|}\right) \quad (1)$$

where N is the number of interacting molecules, and $\mathbf{r}_{ci}$ and $\mathbf{r}_{Di}$ are positions of the core particle i and its Drude particle, respectively. k_θ and θ_0 are the force constant and equilibrium angle for the HSH angles θ. $E_{\min,ij}$ and $R_{\min,ij}$ are the mixed Lennard-Jones (LJ) parameters between nonbonded atoms i and j, defined by the Lorentz−Berthelot combination rules:

$$E_{\min,ij} = \sqrt{E_{\min,i}E_{\min,j}} \quad \text{and} \quad R_{\min,ij} = \frac{R_{\min,i} + R_{\min,j}}{2} \quad (2)$$

Equation 1 does not include bond stretching energy terms since for both water and hydrogen sulfide, bonds are constrained to their equilibrium values using the RATTLE/Roll algorithm.[36] It also does not include HOH angle bending terms since the SWM4-NDP water model has a rigid molecular geometry.[18]

The polarizable model for liquid H_2S is parameterized based on the experimental properties of the gaseous monomer and the density of hydrogen sulfide in the temperature range 363−393 K and pressure range 8.023−10.013 MPa. The model is composed of three atomic sites and a Drude oscillator linked to sulfur. The equilibrium values of the SH bond length and the HSH angle are set to the gas-phase experimental values (r_{SH} = 1.328 Å and θ_{HSH} = 92.2°).[37] The bond and angle force constants, k_b and k_θ, are set to reproduce the experimental vibration frequencies of the monomer. The electrostatic parameters (partial atomic charges and polarizability) are similarly based on the experimental data of the H_2S monomer, with the partial atomic charges on S and H atoms fitted to reproduce the dipole moment, and the polarizability of the S atom set to the polarizability of gaseous H_2S. Compared to previous force fields,[14−17,21] the present model has LJ terms assigned to both sulfur and hydrogen atoms, rather than sulfur only. These parameters are optimized based on the experimental density of the fluid at temperatures 363.25, 373.25, 383.24, and 393.22 K, under pressures of 8.023, 9.344, 10.024, and 10.013 MPa, respectively.[8] Fluid densities calculated with literature models[14−17,21] deviate from experimental data by more than 71% for at least one of these four thermodynamic conditions (see section 3.6.1).

Without specific LJ parameters between S and O and between S and the alkali ions, the model gives relatively poor agreement with the experimental hydration free energy of H_2S and overestimates the CCSD(T) binding energies for H_2S-alkali ion pairs. We therefore adjust the model to reproduce these values by optimizing pair-specific LJ parameters (introduced via the NBFIX[31] facility of CHARMM) between the S atom of H_2S and the O atom of H_2O, and between the S atom and each alkali ion. Optimization of the pair-specific LJ parameters between S and O is done by introducing small changes from the default mixed parameters until the experimental hydration free energy of H_2S is reproduced. Optimization of the pair-specific LJ parameters between S and the alkali ions follows an approach reported elsewhere.[20,24,33−35] Briefly, optimization initially targets the ab initio PESs of the pairs. The obtained parameters are finally adjusted to reproduce the complexation energies of the fully relaxed ab initio pairs while maintaining ion−S separations within 2% of the ab initio CCSD(T) results.[24,33]

2.2.2. Molecular Dynamics. Unless otherwise stated, all MD simulations are performed with cubic periodic boundary conditions in the isothermal−isobaric ensemble (NpT). H_2O molecules are kept totally rigid (bonds and angles) using the RATTLE/Roll algorithm,[36] while only the bonds are kept rigid for H_2S. Simulations of pure liquid H_2S are carried out using 500 molecules at various thermodynamic conditions. To ensure a consistent comparison, all liquid H_2S simulations are repeated using the potential models of Jorgensen,[14] Forester et al.,[15] Kristóf and Liszi,[16] Kamath et al. (model c),[17] and Riahi and Rowley.[21] Except the model of Kamath et al.,[17] which has flexible angles, these models maintain totally rigid H_2S geometries. The solvation structure of water and alkali ions in liquid H_2S is investigated by simulating a single solute (water or alkali ion) in 500 H_2S molecules at the normal boiling point of hydrogen sulfide (T = 212.82 K, p = 0.1013 MPa = 1 atm).[9] For the purpose of comparison, the solvation structure of alkali ions in water is investigated from MD simulations of each alkali ion in 500 water molecules at same thermodynamic conditions (T = 212.82 K, p = 0.1013 MPa). The solvation structure of H_2S in water is investigated from a simulation of one H_2S molecule in 500 H_2O molecules at T = 298.15 K and p = 0.1013 MPa. Calculations of the solvation free energy of the ions in liquid hydrogen sulfide are performed by simulating each ion in 500 H_2S molecules at T = 298.15 K and p = 2.0174 MPa = 19.91 atm (the corresponding vapor pressure of liquid H_2S). Hydrogen sulfide has a very low solubility in water,[38] and thus, we investigate the preferential solvation of alkali ions in aqueous hydrogen sulfide at low mole fraction of H_2S, x_{H_2S} = 0.1. The composition of the aqueous alkali ion solutions is one alkali ion + 450 H_2O molecules + 50 H_2S molecules and the simulations are performed at the boiling point conditions of pure H_2S. It should be noted that water is in the supercooled state during the duration of simulations at 212.82 K.

dx.doi.org/10.1021/ct5002335 | J. Chem. Theory Comput. 2014, 10, 3221−3235

Electrostatic interactions are computed using the particle-mesh Ewald method[39] with $\kappa = 0.34$ for the charge screening and an ~1.0 Å grid spacing with sixth-order splines for the mesh interpolation. The real-space interactions (Lennard-Jones and electrostatic) are cut off at 20 Å and the long-range contribution from the Lennard-Jones term is introduced as an average density-dependent term.[40] A dual Nosé−Hoover thermostat[41] is applied; the first is coupled to the atomic sites to keep temperature at the desired value and the second is coupled to the Drude particles to keep them at low temperature (1 K), to ensure self-consistent dipole induction.[32] The relaxation time of the atomic system is 0.1 ps, while the relaxation time of the Drude system is 0.005 ps. An Andersen−Hoover barostat[42] with a relaxation time of 0.2 ps is used to regulate the pressure. The equations of motion are integrated using a 1 fs time step. Simulations in liquid hydrogen sulfide with and without an alkali ion are run for 10 ns while those in aqueous H_2S are run for 85 ns.

2.2.3. Free Energy Calculations. The intrinsic free energy of solvation of each ion in liquid hydrogen sulfide is calculated at $T = 298.15$ K and $p = 2.0174$ MPa = 19.91 atm, using a free energy perturbation approach reported elsewhere.[20,24] Specifically, the solvation free energy is evaluated from the transformation of one alkali ion, M^+, into a "dummy" atom having no charge and no LJ parameters:

$$\Delta G_{\text{solv}}^{\text{intr}} \equiv \Delta G_{\text{solv}}(M^+) - \Delta G_{\text{solv}}(\text{dummy}) = -\Delta G_{\text{mut}}(M^+ \rightarrow \text{dummy}) \quad (3)$$

where ΔG_{mut} is the relative free energy for the alchemical $M^+ \rightarrow$ dummy "mutation" and $\Delta G_{\text{solv}}(\text{dummy}) = 0$. The transformation is controlled by a scaling parameter λ which takes the following 21 values: 0, 0.00001, 0.0001, 0.001, 0.01, 0.05, 0.1, 0.2, 0.3, 0.4, 0.5, 0.6, 0.7, 0.8, 0.9, 0.95, 0.99, 0.999, 0.9999, 0.99999, and 1.[20,24] Each λ window is equilibrated for 150 ps, and data is collected for 350 ps. Each mutation is performed in the forward and backward directions in three independent replicates. On the basis of multiple runs, the error on the calculated values is ±0.2 kcal/mol. Hydration free energy of H_2S is similarly calculated by mutating H_2S into a dummy molecule in a system of 500 H_2O molecules at $T = 298.15$ K and $p = 0.1013$ MPa.

2.2.4. Calculation of Thermodynamic and Transport Properties. Thermodynamic and transport properties are calculated for all H_2S models and compared to experimental values. The enthalpy of vaporization, ΔH_{vap}, is calculated from the net gain of potential energy Δu upon formation of the dense system.[20]

$$\Delta H_{\text{vap}} = p(\langle V\rangle_g - \langle V\rangle_l) + (\langle u\rangle_g - \langle u\rangle_l) \quad (4)$$

where p is the pressure, $\langle V\rangle_g$ and $\langle V\rangle_l$ are the average molar volumes of gaseous and liquid H_2S, and $\langle u\rangle_g$ and $\langle u\rangle_l$ are the average potential energies of the two phases. $\langle V\rangle_l$ and $\langle u\rangle_l$ are obtained from the NpT MD simulations, $\langle V\rangle_g$ is taken from the NIST Chemistry webBook,[13] and $\langle u\rangle_g$ is obtained from MD simulations of 500 H_2S molecules in the NVT ensemble at a volume consistent with $\langle V\rangle_g$.

The self-diffusion coefficient of an H_2S molecule in the liquid state is obtained from the long-time limit of the mean-square displacement of the sulfur atoms:[20]

$$D_{\text{PBC}} = \lim_{t\rightarrow\infty} \frac{1}{6t} \left\langle \frac{1}{N} \sum_{i=1}^{N} [\mathbf{r}_{S,i}(t) - \mathbf{r}_{S,i}(0)]^2 \right\rangle \quad (5)$$

The resulting diffusion coefficient, obtained from a least-squares linear fit of each successive 2 ns of the last 8 ns of the trajectories, is corrected for system-size dependence using the formula of Yeh and Hummer:[43]

$$D = D_{\text{PBC}} + \frac{2.837297 k_B T}{6\pi\eta L} \quad (6)$$

where k_B is Boltzmann constant, η the shear viscosity of the solvent, and L is the average length of the cubic simulation box.[43] The viscosity values of liquid H_2S at the simulated thermodynamic conditions are taken from the NIST Chemistry webBook.[13]

The dielectric constant of the liquid, ε, was calculated using[44]

$$\varepsilon = \varepsilon_\infty + \frac{4\pi}{3\langle V\rangle k_B T}(\langle \mathbf{M}\rangle^2 - \langle \mathbf{M}\rangle^2) \quad (7)$$

where $\mathbf{M}$ is the total dipole moment of the box and ε_∞ is infinite-frequency dielectric constant, estimated from the Clausius−Mossotti equation (see, e.g., ref 45):

$$\frac{\varepsilon_\infty - 1}{\varepsilon_\infty + 2} = \frac{4\pi\alpha}{3v} \quad (8)$$

where α is the molecular polarizability and v is the molecular volume obtained from the simulation. The convergence of ε is monitored by plotting its value as a function of time and is averaged over the last 7 ns of 10 ns long simulations.

The specific heat capacity at constant pressure (C_p) is calculated from five simulations at different temperatures, 192.82, 197.82, 202.82, 207.82, and 212.82 K and at a constant pressure of 0.1013 MPa. The total energy U_{tot} and the volume V are averaged over time. A linear fit of the plot $(U_{\text{tot}} + pV)$ versus T is used to calculate C_p.[20]

$$C_p = \frac{1}{N}\left(\frac{\partial(\langle U_{\text{tot}}\rangle + p\langle V\rangle)}{\partial T}\right)_{T=212.82\text{K},p=0.1013\text{Pa}} \quad (9)$$

3. RESULTS AND DISCUSSION

3.1. Ab Initio Optimized Geometries. Due to the limited number of ab initio investigations on H_2S-containing clusters in the literature,[14,21] we report all stable conformers we have identified. To the best of our knowledge, ab initio investigations on H_2S clusters larger than the dimer and on clusters of H_2S with alkali ions (other than the Na^+−H_2S dimer[14]) have not been reported so far.

3.1.1. Hydrogen Sulfide Monomer. The MP2/6-311++G(d,p) calculated equilibrium geometry, dipole moment, polarizability, and vibrational frequencies of the isolated hydrogen sulfide molecule are reported in Table 1, together with the corresponding experimental and Drude values. The geometry of H_2S optimized at the MP2 level shows $r_{SH} = 1.333$ Å and $\theta_{HSH} = 92.0°$, in agreement with the experimental data ($r_{SH} = 1.328$ Å, $\theta_{HSH} = 92.2°$).[37] In comparison, the equivalent parameters for water are $r_{OH} = 0.958$ Å and $\theta_{HOH} = 104.5°$,[46] showing the effect of the larger 3p orbitals on the structure of H_2S. The MP2-optimized structure possesses a dipole moment of 1.37 D, larger than the experimental gas-phase value (0.97 D).[47] Table 1 also shows that, compared to the experimental values,[48,49] the calculated polarizability is underestimated while

Table 1. Ab Initio Calculated Properties of the Hydrogen Sulfide Monomer at the MP2/6-311++G(d,p) Level and Corresponding Experimental Values[a]

property	ab initio	Drude	expt.
SH bond length (Å)	1.333	1.328	1.328[b]
HSH angle (deg)	92.0	92.2	92.2[b]
dipole (D)	1.37	0.97	0.97[c]
polarizability (α, Å^3)	2.651	3.631	3.631[d]
vibration frequencies (cm^{-1})			
ν_1	1233	1183	1183[e]
ν_2	2819	2621	2615[e]
ν_3	2839	2624	2626[e]

[a]Values from the optimized Drude model are also given. [b]Ref 37. [c]Ref 47. [d]Ref 48. [e]Ref 49.

the calculated frequencies are overestimated. The trend in the experimental polarizability, H_2O (1.501 Å^3) < NH_3 (2.103 Å^3) < H_2S (3.631 Å^3),[48] reflects the increase in molecular volume. Since MP2 calculations do not adequately reproduce the experimental values, the bonded parameters and the atomic charges of the Drude model are adjusted based on the experimental parameters.

3.1.2. $(H_2S)_n$ (n = 2–4) Clusters. Figure 1 shows structures of the $(H_2S)_n$ clusters (n = 2–4) obtained from geometry

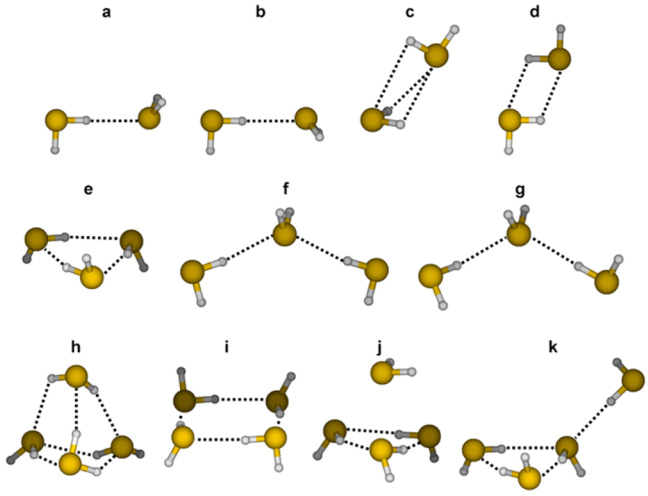

Figure 1. Geometries of hydrogen sulfide clusters optimized at the MP2/6-311++G(d,p) level: (a–d) dimer, (e–g) trimer, and (h–k) tetramer. Structure **d** is a transition state.

optimization at the MP2/6-311++G(d,p) level. Table 2 lists the interaction energies of four structures of the dimer calculated at the same level and at MP2/aug-cc-pVXZ levels (X = D, T, Q, and 5). Table 3 reports the MP2/6-311++G(d,p) interaction energies of the optimized structures of the trimer and tetramer clusters. Ab initio interaction energies are reported with and without correction for BSSE (E^{CP} and E, respectively). Interaction energies from the optimized Drude model are reported in Tables 2 and 3, along with energies from potential models from the literature[14−17,21] (recalculated in this work).

Geometry optimization of the dimer reveals three stable structures (**a**–**c**) and a TS structure (**d**). Structures **a** and **b** form linear hydrogen-bonds with intermolecular distances $r_{S\cdots H}$ and angles $\theta_{S-H\cdots S}$ of 2.838 Å and 178.2° for complex **a** and of 2.833 Å and 177.0° for complex **b**. Structure **c** is cyclic,

Table 2. Uncorrected (E) and CP-Corrected (E^{CP}) Binding Energies of the Hydrogen Sulfide Dimer, $(H_2S)_2$, Calculated at the MP2 Level at Various Basis Sets[a]

	ab initio, MP2/								potential models[b]				
	6-311++G(d,p)		aug-cc-pVDZ		aug-cc-pVTZ		aug-cc-pVQZ		aug-cc-pV5Z						
structure	E	E^{CP}	E	E^{CP}	E	E^{CP}	E	E^{CP}	E	E^{CP}	$E^{MM,c}$	$E^{MM,d}$	$E^{MM,e}$	$E^{MM,f}$	$E^{MM,g}$	$E^{MM,h}$
a (trans)	−2.25	−0.87	−2.73	−1.50	−2.95	−1.66	−2.26	−1.83	−2.42	−1.83	−1.79	−1.37	−1.35	−1.47	−0.95	−0.93
b (cis)	−2.17	−0.80	−2.63	−1.41	−2.87	−1.59	−2.17	−1.74	−2.35	−1.75	−1.23	−1.22	−1.16	−1.10	−0.85	−0.81
c (cyclic)	−1.99	−0.73	−2.14	−1.42	−2.33	−1.65	−2.09	−1.80	−2.21	−1.84	−1.63	−0.87	−0.82	−1.14	−0.50	−0.58
d (TS)	−1.85	−0.76	−2.15	−1.35	−2.41	−1.51	−2.00	−1.66	−2.10	−1.69	−1.41	−0.94	−0.87	−1.05	−0.57	−0.56

[a]Binding energies calculated with potential models of H_2S are also reported. All energies are in kcal/mol. [b]Binding energies are calculated on the MP2/6-311++G(d,p) optimized geometries. [c]Jorgensen model.[14] [d]Forester et al. model.[15] [e]Kristóf and Liszi model.[16] [f]Model C of Kamath et al.[17] [g]Riahi and Rowley Drude model.[21] [h]This work.

dx.doi.org/10.1021/ct5002335 | J. Chem. Theory Comput. 2014, 10, 3221−3235

Table 3. Uncorrected (E) and CP-Corrected (E^{CP}) Binding Energies of the $(H_2S)_n$ Clusters (n = 3, 4) Calculated at the MP2/6-311++G(d,p) Level[a]

	ab initio		potential models					
conformer	E	E^{CP}	Jorgensen[14]	Forester et al.[15]	Kristóf and Liszi[16]	Kamath et al.[17]	Riahi and Rowley[21]	this work
e	−6.22	−2.74	−4.65	−4.13	−3.92	−3.91	−2.74	−2.72
f	−4.27	−1.66	−3.16	−2.66	−2.57	−2.67	−1.82	−1.80
g	−4.23	−1.57	−2.86	−2.58	−2.47	−2.48	−1.76	−1.72
h	−10.47	−4.48	−7.67	−6.88	−6.52	−6.66	−4.91	−5.03
i	−10.09	−4.33	−7.32	−6.26	−6.00	−6.09	−4.38	−4.51
j	−10.26	−3.97	−3.79	−4.39	−3.70	−3.41	−3.83	−3.80
k	−8.71	−3.67	−6.31	−5.55	−5.28	−5.31	−3.82	−3.81

[a]Binding energies calculated with the optimized Drude model and with other literature models are also reported. Binding energies are calculated on the MP2/6-311++G(d,p) optimized geometries of the trimers and tetramers. All energies are in kcal/mol.

stabilized by the interaction of hydrogen atoms with electron lone pairs on sulfur, and displays $r_{S\cdots H}$ separations of 3.30 and 3.69 Å. The TS structure **d** is also cyclic, with equal $r_{S\cdots H}$ distances of 3.286 Å and $\theta_{S-H\cdots S}$ angles of 102.7°. The dihedral angle $d_{H-S-H\cdots S}$ in structure **d** is 138°. S···S distances are 4.172 Å for conformer **a**, 4.166 Å for **b**, 3.770 Å for **c**, and 3.808 Å for **d**. Table 2 shows that, while the CP-uncorrected binding energies are comparable for MP2/6-311++G(d,p) and MP2/aug-cc-pVXZ levels, they are significantly different after CP correction.

The trimer, $(H_2S)_3$, has three stable conformations: **e**, **f**, and **g** (see Figure 1 and Table 3). Structure **e** is cyclic with two hydrogen bonds per H_2S molecule. Structures **f** and **g** differ only in the orientation of the terminal H atoms (cis in **f** and trans in **g**). The binding energies of these conformers follow the order **e** > **f** > **g** (in absolute value).

Figure 1 shows four conformers for the tetramer, $(H_2S)_4$. The global energy minimum is conformer **h**, in which three H_2S molecules are hydrogen-bonded in a cyclic form and each is involved in a single hydrogen bond with the fourth molecule. Conformer **i** is cyclic planar with two hydrogen bonds per H_2S molecule. Conformer **j** is structurally similar to **h**, but has no apparent hydrogen bonding between molecules in the cyclic trimer and the fourth one. Structure **k** corresponds to a cyclic trimer hydrogen-bonded to a fourth molecule through a single hydrogen bond. The binding energies of these four tetramers follow the order **h** > **i** > **j** > **k** (in absolute value).

3.1.3. H_2S–H_2O Dimer. Figure 2 shows structures of the H_2S–H_2O pair optimized at the MP2/6-311++G(d,p) level. The corresponding ab initio binding energies (E and E^{CP}) and the Drude-calculated values (E^{MM}) are reported in Table 4.

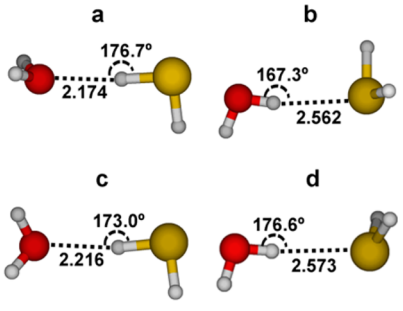

Figure 2. Geometries of the H_2S–H_2O pair optimized at the MP2/6-311++G(d,p) level. Structures **a** and **b** are energy minima and structures **c** and **d** are transition states. Hydrogen bond distances (in Å) and angles are reported.

Table 4. Uncorrected (E) and CP-Corrected (E^{CP}) Binding Energies of the H_2S–H_2O Pair, Calculated at the MP2/6-311++G(d,p) Level[a]

structure	E	E^{CP}	E^{MM}*
a	−3.71	−2.33	−1.28
b	−3.40	−1.94	−1.53
c	−3.31	−2.03	−1.33
d	−3.38	−1.91	−1.58

*Binding energies are calculated on the MP2/6-311++G(d,p) optimized geometries of the dimer. [a]Binding energies calculated with the optimized Drude model (E^{MM}) are also reported. All energies are in kcal/mol.

Structure **a** is the global energy minimum, with a linear hydrogen bond in which water is the proton acceptor. Structure **b** forms a hydrogen bond in which water is the proton donor. Conformers **c** and **d** are hydrogen-bonded TS structures in which water is the proton acceptor and donor, respectively. Intermolecular $r_{S\cdots O}$ distances for structures **a**, **b**, **c**, and **d** are 3.509, 3.507, 3.546, and 3.534 Å, respectively.

3.1.4. H_2S–Alkali Ion Pairs. Figure 3 reports the structures of the H_2S–M^+ pairs (M^+ = Li^+, Na^+, K^+, Rb^+, Cs^+) optimized

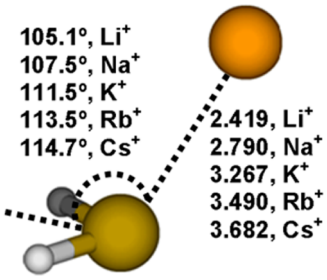

Figure 3. Optimized geometry of the H_2S–K^+ pair optimized at the CCSD(T) level (see Methods section for details). Bond lengths (in Å) and bond angles are reported for all ions.

at the CCSD(T) level. The structures have a C_s point-group symmetry, with both intermolecular distances $r_{S\cdots M^+}$ and angles $\theta_{M^+\cdots S\cdots Y}$, (where Y is a point on the HSH angle bisector) increasing in going from Li^+ to Cs^+. Binding energies calculated at the MP2 and CCSD(T) levels are in close agreement (see Table 5). The Drude model for H_2S–alkali ions interactions is optimized to reproduce binding energies at the CCSD(T) level, and energies calculated with the model (E^{MM}) are reported in Table 5.

dx.doi.org/10.1021/ct5002335 | J. Chem. Theory Comput. 2014, 10, 3221−3235

Table 5. Uncorrected (E) and CP-Corrected (E^{CP}) Binding Energies of the Ion−H_2S Pairs Calculated at the MP2 and CCSD(T) Levels[a]

	ab initio				
	MP2		CCSD(T)		Drude model
ion	E	E^{CP}	E	E^{CP}	E^{MM}*
Li^+	−25.13	−22.08	−23.57	−22.24	−22.20
Na^+	−16.17	−13.97	−16.21	−14.72	−14.70
K^+	−10.27	−9.12	−10.09	−9.47	−9.50
Rb^+	−8.50	−8.16	−8.24	−7.88	−7.90
Cs^+	−7.58	−7.23	−7.33	−6.86	−6.90

[a]See Methods section for details. Binding energies calculated with the optimized Drude model (E^{MM}) are also reported. All energies are in kcal/mol. *Binding energies are calculated without geometry constraints (except for S−H bond lengths which are fixed to their equilibrium value).

3.2. Potential Energy Surfaces. Ab initio potential energy curves for H_2S in complex with H_2S, H_2O, and alkali ions are reported in Figure 4, along with the corresponding curves calculated with the Drude model. Three curves (Figure 4a−c) are calculated for the hydrogen sulfide dimer by rigidly translating the individual molecules along the S−S axis, starting from the optimized dimer structure (structures **a**−**c** of Figure 1) from 2 to 10 Å. Similarly, three potential energy curves are calculated for the H_2S−H_2O pair (Figure 4d−f) by scanning the S···O distance in three optimized structures of the pair (structures **a**, **b**, and **c** in Figure 2). Two curves are calculated for the H_2S−alkali ion pairs: the curve in Figure 4g is obtained by scanning the distance between the alkali ion and the sulfur atom of H_2S from 2 to 10 Å, and the curve in Figure 4h is calculated by scanning the M···S···Y angle from 0° to 180°. In all distance scans, H_2S and H_2O fragments are set to their optimized monomer geometries and the distance between the heavy atoms is changed.

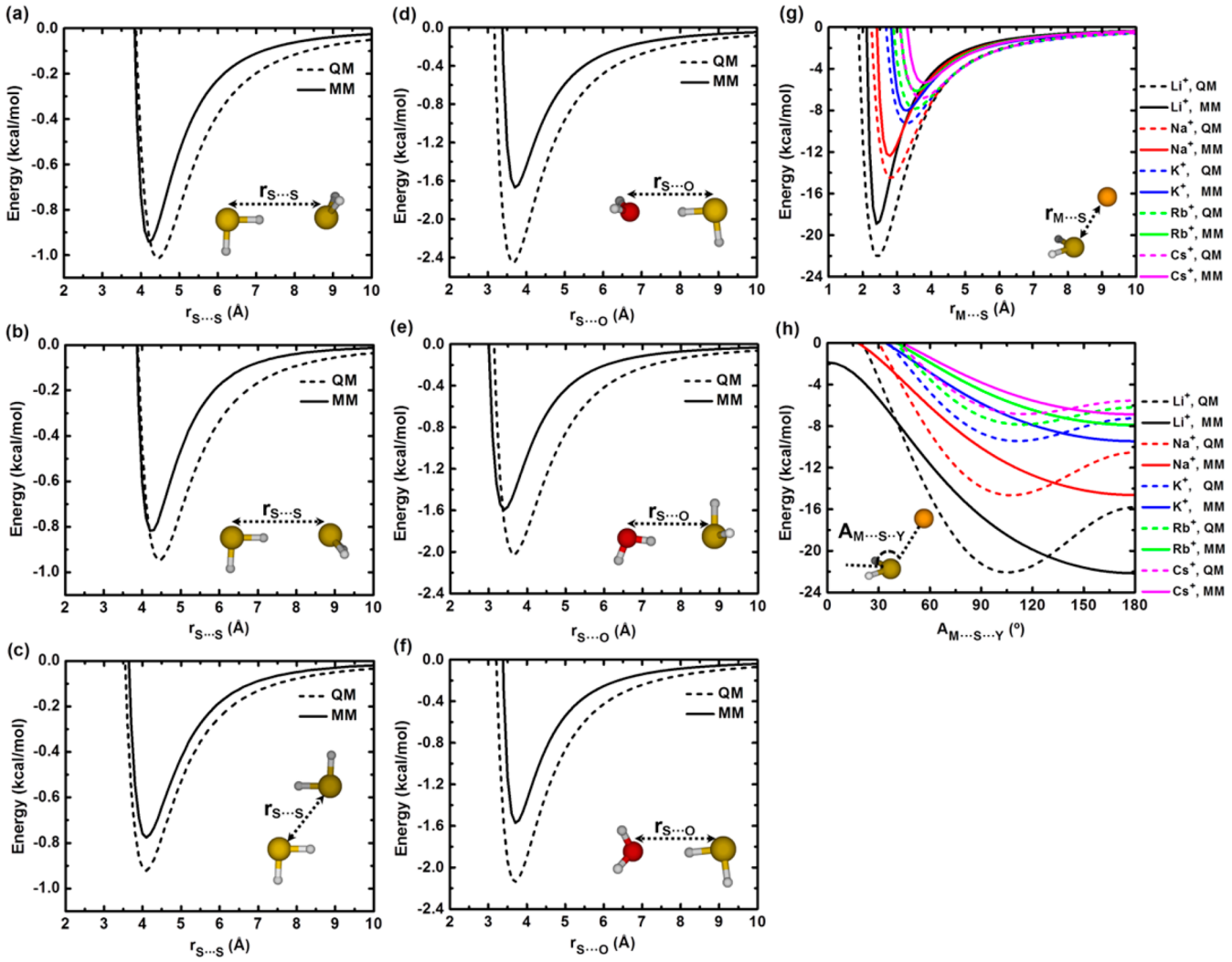

Figure 4. Potential energy curves for H_2S−H_2S, H_2S−H_2O, and H_2S−alkali ions complexes from ab initio calculations (dashed lines) and from the polarizable model (solid lines). Curves a−c are calculated by scanning the S···S distance in the three stable conformers of the H_2S dimer (structures **a**−**c** of Figure 1) from 2 to 10 Å. Curves d−f are calculated by scanning the S···O distance in three conformers of the H_2S−H_2O dimer (structures **a**−**c** of Figure 2) from 2 to 10 Å. The curve in part g is calculated by scanning the ion−S distance from 2 to 10 Å. The curve in part h is obtained by scanning the M···S···Y angle (Y is a point on the HSH angle bisector) from 0 to 180° at M···S distances of 2.4 Å for Li^+, 2.8 Å for Na^+, 3.3 Å for K^+, 3.5 Å for Rb^+, and 3.7 Å for Cs^+.

dx.doi.org/10.1021/ct5002335 | J. Chem. Theory Comput. 2014, 10, 3221−3235

Table 6. Parameters of the Optimized H_2S Model, Compared to Models from the Literature[a]

param.	Jorgensen[14]	Forester et al.[15]	Kristóf and Liszi[16]	Kamath et al.[17]	Riahi and Rowley[21]	this work
r_{SH} (Å)	1.340	1.3322	1.340	1.340	1.340	1.328
θ_{HSH} (deg)	92.0	92.1	92.0	92.5	92.0	92.2
r_L (Å)		0.1933	0.1862		0.2020	
q_S (e)	−0.470	0.661	0.400	−0.380	0.000	−0.220
q_H (e)	0.235	0.278	0.250	0.190	0.137	0.110
q_L (e)		−1.217	−0.900		−0.274	
α (Å^3)					2.500	3.631
$E_{min,\,S}$ (kcal/mol)	0.2501	0.5346	0.4969	0.4611	0.5681	0.304738
$R_{min,\,S}/2$ (Å)	2.0766	2.0709	2.0933	2.0878	2.088	2.174804
$E_{min,\,H}$ (kcal/mol)						0.157138
$R_{min,H}/2$ (Å)						0.808847

[a] r_L is the distance between the sulfur atom and the lone pair on the bisector of the HSH angle and q_L is the lone pair charge.

Table 7. Pair-Specific LJ Parameters between the S Atom of H_2S and Alkali Ions and between S and O of Water

param.	Li^+	Na^+	K^+	Rb^+	Cs^+	H_2O
$E_{min,\,ion-s}$ (kcal/mol)	0.161863	0.184228	0.286566	0.454744	0.515176	0.273540
$R_{min,\,ion-s}/2$ (Å)	1.719424	1.859696	2.024616	2.092886	2.179827	1.937867

Table 8. Liquid Properties of H_2S Models at 212.82 K and 0.1013 MPa = 1 atm, and Corresponding Experimental Values[a]

model	ρ (kg/m^3)	ΔH_{vap} (kcal/mol)	$D \times 10^{-9}$ m^2/s	ε	C_p (cal mol^{-1} K^{-1})
Jorgensen[14]	0.958 ± 0.001	4.79 ± 0.01	8.52 ± 0.1	48.8 ± 1.0	10.2 ± 0.2
Forester et al.[15]	1.016 ± 0.001	4.28 ± 0.01	3.01 ± 0.1	9.5 ± 0.2	9.7 ± 0.2
Kristóf and Liszi[16]	0.958 ± 0.001	4.43 ± 0.01	3.81 ± 0.1	11.6 ± 0.2	9.4 ± 0.2
Kamath et al.[17]	0.958 ± 0.001	4.36 ± 0.01	4.37 ± 0.1	24.5 ± 0.2	10.4 ± 0.2
Riahi and Rowley[21]	0.952 ± 0.001	4.34 ± 0.01	3.34 ± 0.1	7.6 ± 0.1	8.4 ± 0.2
this work	0.912 ± 0.001	3.87 ± 0.01	3.62 ± 0.1	8.9 ± 0.1	10.2 ± 0.2
expt.[b]	0.949	4.46	3.7 ± 0.2	8.04	16.31

[a] All properties are calculated in this work. [b] Density and enthalpy of vaporization from ref 7, self-diffusion coefficient from ref 11 at 206.5 K, dielectric constant from ref 12, and heat capacity from ref 9 at 211 K.

3.3. Optimized Force Field. The optimized parameters of the polarizable Drude model as well as parameters from previous potential models[14−17,21] are reported in Table 6. The equilibrium structural parameters for the H_2S model are set to the experimental data: r_{SH} = 1.328 Å and θ_{HSH} = 92.2°. The corresponding force constants, k_b = 285.0 kcal/mol·Å^2 and k_θ = 51.1 kcal/mol·rad^2, are chosen to reproduce the experimental vibration frequencies (see Table 1). The isotropic Drude polarizability is set to the experimental molecular polarizability and the partial atomic charges are set to reproduce the experimental dipole moment of gaseous H_2S. The LJ parameters for S and H are optimized based on the experimental density of H_2S at four thermodynamic conditions around the critical point, in the temperature range 363−393 K and pressure range 8.023−10.013 MPa. The four LJ parameters are chosen to minimize deviations from the experimental density values at those four thermodynamic conditions.

LJ parameters for the S−O pair are optimized to reproduce the experimental hydration free energy of H_2S; for the S−alkali ion pairs, they are optimized to reproduce the CCSD(T)-calculated binding energies and the ion−S distances of the H_2S−ion pairs. Adjusted pair-specific LJ parameters are reported in Table 7.

Except for the binding energies of alkali ions−H_2S pairs, which are calculated using the force field-optimized geometries, binding energies of hydrogen sulfide clusters (Figure 1) and of H_2S−H_2O pairs (Figure 2) are calculated using the MP2-optimized geometries.

Despite not being optimized to reproduce the ab initio properties of the clusters, the model shows only minor deviations from the ab initio H_2S−H_2S PESs (see Figure 4a−c). Moreover, the Drude models for H_2S (this work and that of Riahi and Rowley[21]) give binding energies for the various hydrogen sulfide clusters in good agreement with ab initio data at the MP2/6-311++G(d,p) level (see Tables 2 and 3). In comparison the additive models of Jorgensen,[14] Forester et al.,[15] Kristóf and Liszi,[16] and Kamath et al. (model C)[17] overestimate the CP-corrected binding energies at the MP2 level.

The Drude model for the H_2S−H_2O pair, which is adjusted to reproduce the hydration free energy of H_2S and not the ab initio properties of the pair, underestimates the ab initio binding energy (see Table 4 and Figure 4d−f). While MP2 results predict hydrogen-bonded structures in which H_2S is the proton donor (Figure 2a, c) to be slightly more stable than those in which H_2O is the proton donor (Figure 2b, d), the model is showing the opposite trend.

When using the Lorentz−Berthelot combination rules, the Drude models of H_2S and alkali ions[26] give binding energies for the alkali ion−H_2S pairs of −34.30 kcal/mol for Li^+, −20.14 kcal/mol for Na^+, −12.42 kcal/mol for K^+, −10.47 kcal/mol for Rb^+, and −8.50 kcal/mol for Cs^+. These values are greatly overestimated compared to the ab initio CCSD(T) binding energies (see Table 5). With pair-specific LJ parameters between the sulfur atom of H_2S and each alkali ion (see Table 7), the model reproduces the CCSD(T) binding energies

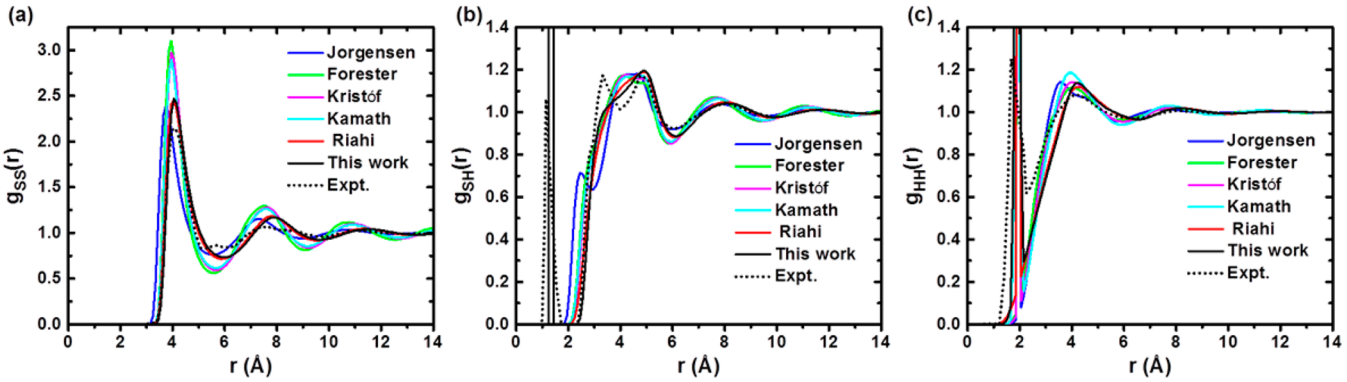

Figure 5. $g_{SS}(r)$, $g_{SH}(r)$, and $g_{HH}(r)$ radial distribution functions of liquid hydrogen sulfide at T = 298 K and p = 3.1 MPa calculated from D simulation using different potential models (solid lines) in comparison with NDIS experiment[6] at the same conditions (dashed lines).

of the ion−H_2S pairs and gives ion−S separations of 2.416 Å for Li^+, 2.761 Å for Na^+, 3.246 Å for K^+, 3.533 Å for Rb^+, and 3.756 Å for Cs^+, in good agreement with the ab initio data at the CCSD(T) level (see Table 5 and Figure 3). The model, however, gives a C_{2v} symmetry for all H_2S−ion pairs, with an M···S···Y angle of 180°. Reproducing the ab initio observed C_s symmetry of the pairs may require explicit description of the lone pairs of the S atom. The Drude model of Riahi and Rowley[21] possesses a "lone pair" site on the bisector of the HSH angle, yet gives a C_{2v} symmetry as well. Two lone pair sites might thus be required to mimic the tetrahedral electron-pair geometry of H_2S and reproduce the ab initio geometries of its complexes with ions.

3.4. Liquid Hydrogen Sulfide at the Boiling Point. The Drude model is used to calculate properties of liquid hydrogen sulfide at its normal boiling point (T = 212.82 K and p = 0.1013 MPa = 1 atm):[9] density (ρ), heat of vaporization (ΔH_{vap}), self-diffusion coefficient (D), dielectric constant (ε), and heat capacity (C_p) (see Table 8). For consistent comparison, the same properties are recalculated for all literature models.,[14−17] For nonpolarizable models from the literature, the values we find are in good agreement with those reported by Riahi and Rowley.[21] The present polarizable model yields an average molecular volume of 62.04 Å^3 and a density of 0.912 ± 0.001 g/cm^3. By comparison, simulation of 500 H_2O molecules using the SWM4-NDP model[18] at the same thermodynamic conditions yields an average molecular volume of 28.70 Å^3 and a density of 1.042 g/cm^3. The densities calculated from the various models are in good agreement with the experimental value. The maximum deviation from experiment is observed for Forester et al.'s model,[15] which overestimates the experimental value by 7%. Enthalpies of vaporization from the various models are also in good agreement with the experimental value, with a maximum deviation of 0.59 kcal/mol for the current model. The experimental value of the self-diffusion coefficient (at 206.5 K)[11] is best reproduced by our model and that of Kristóf and Liszi.[16] The models of Forester et al.[15] and of Riahi and Rowley[21] underestimate D by 19% and 10%, respectively, while the models of Jorgensen[14] and of Kamath et al.[17] overestimate it. The dielectric constant is best reproduced by the two polarizable models. Other models[14−17] overestimate it by anywhere from 44%[15] to ∼500%.[14] All models of H_2S underestimate the experimental heat capacity of the liquid, likely in part because they use H_2S molecules that are either totally rigid or that have flexible angles but rigid bonds lengths.

3.5. Structure of Liquid H_2S. To investigate the microscopic structure of liquid hydrogen sulfide, we simulate a system of 500 H_2S molecules for all models presented.[14−17,21] Simulations are performed at T = 298 K and p = 3.1 MPa = 30.595 atm, one of the experimental thermodynamic conditions reported by Santoli et al.[6] The structure of the liquid is analyzed from the $g_{SS}(r)$, $g_{SH}(r)$, and $g_{HH}(r)$ radial distribution functions (RDFs), shown in Figure 5. The characteristic properties of the $g_{SS}(r)$ function are reported in Table 9.

Except for Jorgensen's model,[14] the position of the first peak in the $g_{SS}(r)$ function is in good agreement with the experimental value (∼4 Å).[6] Compared to experiment, the intensity of the first peak in the calculated function is overestimated, especially for models of Forester et al.,[15] Kristóf and Liszi,[16] and Kamath et al.[17] Such overestimation is likely due to the steepness of the Lennard-Jones repulsive potential.[20] The two Drude models show the first minimum in the $g_{SS}(r)$ function at relatively longer distances compared to the pairwise-additive models. The present model predicts the lowest coordination number of all: 11.3 hydrogen sulfide molecules, compared to 12.0 for the Riahi and Rowley model.

The first peak in the $g_{SH}(r)$ function, located at r < 2 Å, corresponds to intramolecular SH pairs. Among all models, only the Jorgensen model suggests clear hydrogen bonding in liquid H_2S (evidenced by the peak centered at 2.5 Å), which is inconsistent with experiment. The present model is the most accurate in reproducing the features of the experimental $g_{SH}(r)$ function; it correctly reproduces the double peaks at ∼3.2 Å and ∼4.8 Å in the experimental function.[6] The peak at ∼3.2 Å is consistent with the distance of 3.3 Å in structures 1**c** and 1**d** of the dimers (see section 3.1). It should also be noted that the very weak shoulder at ∼2.8 Å in the experimental curve of Figure 5b is consistent with the distance found in the linearly hydrogen-bonded dimers (structures 1**a** and 1**b** of Figure 1). δThe absence of an intense peak in the $g_{SH}(r)$ function at a distance characteristic of any specific binding geometry, and hence for the observed structureless pattern might be explained by the fact that the four optimized structures of the dimer (1**a** to 1**d**) have comparable energies despite the broad $r_{S\cdots H}$ range covered (from 2.83 to 3.69 Å). However, since the four optimized structures are characterized by hydrogen bonding features, hydrogen bonding in liquid H_2S may still persist.

The $g_{HH}(r)$ function shows a first peak at 1.9 Å, due to intramolecular HH pairs. With the exception of Jorgensen's model,[14] the position of the experimental first intermolecular peak (∼4.2 Å)[6] is well reproduced by the different models.

dx.doi.org/10.1021/ct5002335 | J. Chem. Theory Comput. 2014, 10, 3221−3235

3.6. Liquid H_2S at Various p and T. The transferability of the optimized Drude model for H_2S is validated by calculating the density, vaporization enthalpy, and self-diffusion coefficient of H_2S at thermodynamic conditions that cover the liquid and supercritical phases of the fluid. Figure 6 summarizes the temperature and pressure conditions simulated.

Table 9. Characteristics of the $g_{SS}(r)$ Radial Distribution Function of Liquid Hydrogen Sulfide at T = 298 K and p = 3.1 MPa[a]

model	r_{M1} (Å)	r_{m1} (Å)	$n(r_{m1})$	r_{M2} (Å)
Jorgensen[14]	3.75	5.55	11.9	7.30
Forester et al.[15]	3.95	5.55	12.7	7.55
Kristóf and Liszi[16]	3.95	5.65	12.6	7.65
Kamath et al.[17]	3.95	5.65	12.6	7.65
Riahi and Rowley[21]	4.05	5.90	12.0	7.75
this work	4.05	5.90	11.3	7.85

[a] r_{M1} and r_{M2} are the distances at which the function has its first and second maximum, respectively. r_{m1} is the distance at which the function has its first minimum and $n(r_{m1})$ is the running integration number evaluated at r_{m1}.

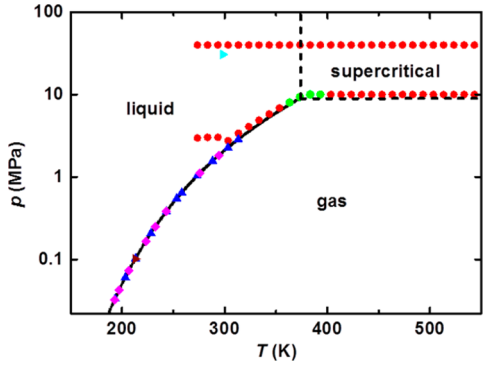

Figure 6. Phase diagram of H_2S. The solid and dashed lines are phase boundaries and their intersection is the critical point (T_c = 373.1 K, p_c = 9.00 MPa).[13] Green circles are the pressure and temperature conditions used to optimize the LJ parameters for H and S atoms. Red circles are the conditions at which density is investigated (see Table S1 of Supporting Information (SI)). Blue triangles are conditions at which vaporization enthalpy is investigated (see Table S2 of SI). Pink diamonds are conditions at which self-diffusion coefficient is investigated (see Table S3 of SI). The brown triangle represents the normal boiling point of H_2S (T = 212.82 K, p = 0.1013 MPa = 1 atm),[9] and the cyan triangle represents one of Santoli et al.'s NDIS experimental conditions[6] (T = 298 K, p = 3.1 MPa = 30.595 atm), at which liquid structure is calculated.

3.6.1. Density. Ihmels and Gmehling[8] have measured the density of H_2S in the liquid and supercritical phases in the temperature range 273.39−548.30 K and in the pressure range 2.976−40.004 MPa. To validate the optimized model and to test the performance of models from the literature,[14−17,21] a system of 500 H_2S molecules is simulated for 10 ns at temperatures from ∼273 K to ∼543 K in 10 K increments. For each temperature, the system is simulated at two pressures that correspond to the minimum and maximum pressures used by Ihmels and Gmehling[8] (the red and green symbols in Figure 6). Figure 7 shows calculated versus experimental densities (see also Table S1, SI). Over the 56 simulated conditions, the average unsigned relative error on the density is 1.9% for the present Drude model, 13.7% for the Drude model of Riahi and Rowley,[21] and 15.0%, 23.2%, 6.1%, and 5.4% for the additive models by Jorgensen,[14] Forester et al.,[15] Kristóf and Liszi,[16] and Kamath et al.,[17] respectively. The present model, optimized at temperatures 363.25, 373.25, 383.24, and 393.22 K, under corresponding pressures of 8.023, 9.344, 10.024, and 10.013 MPa (green circles in Figure 6), gives the best agreement with experimental data. Throughout all simulated conditions, the only significant deviation (15.2% overestimation) between experimental and calculated densities is at T = 373.25 K and p = 9.344 MPa, near the critical point of H_2S (T = 373.2 K and p = 8.937 MPa,[8] see Figure 6). Figure 7 shows that other models deviate appreciably from experiment at certain thermodynamic conditions. The Drude model of Riahi and Rowley[21] and the pairwise-additive models of Forester et al.,[15] Kristóf and Liszi,[16] and Kamath et al.[17] largely overestimate the density at low pressure conditions, in the temperature range 353−403 K. On the other hand, the additive model of Jorgensen underestimates the density in the temperature range 313−383 K, suggesting that the liquid−vapor phase boundary has been crossed.

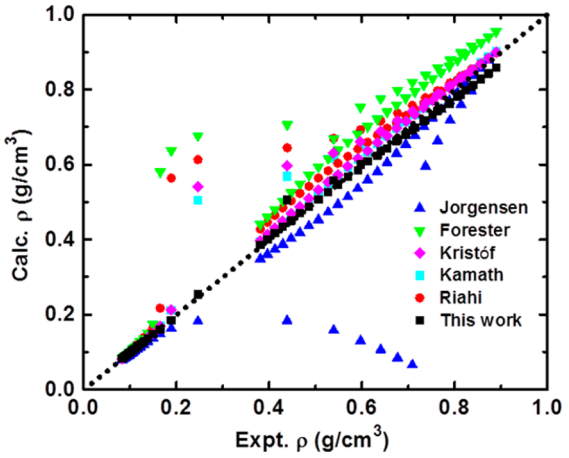

Figure 7. Calculated versus experimental[8] densities of fluid hydrogen sulfide under the thermodynamic conditions shown in red in Figure 6 (also reported in Table S1). The dotted line represents the equation Calc. ρ = Expt. ρ.

3.6.2. Vaporization Enthalpy. Figure 8 shows the temperature dependence of the vaporization enthalpy of liquid H_2S in the temperature range 193−313 K of the vapor−liquid

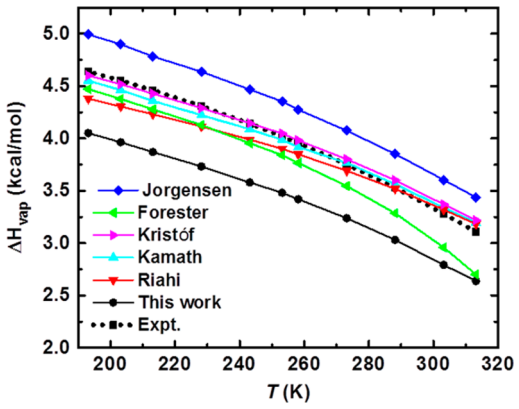

Figure 8. Enthalpy of vaporization of H_2S calculated with the present model and with models from the literature[14−17,21] in the temperature range 193.15−313.15 K, along the liquid−vapor coexistence curve. Experimental values are from ref 7.

dx.doi.org/10.1021/ct5002335 | J. Chem. Theory Comput. 2014, 10, 3221−3235

coexistence curve (see Table S2, SI for tabulated data). The potential models of Kristóf and Liszi,[16] and of Kamath et al.[17] show the best agreement with experiment. While the current model systematically underestimates the calculated vaporization enthalpies by ~0.5 kcal/mol, Jorgensen's model[14] overestimates it by ~0.3 kcal/mol. The Drude model of Riahi and Rowley[21] shows good agreement with experiment at high temperature. The model of Forester et al.[15] underestimates the vaporization enthalpies by an amount that increases with temperature.

3.6.3. Self-Diffusion Coefficient. Self-diffusion coefficients are calculated along the liquid−vapor coexistence curve, in the temperature range 192.8−294.1 K, using a system of 500 H_2S molecules. Figure 9 shows the temperature dependence of the

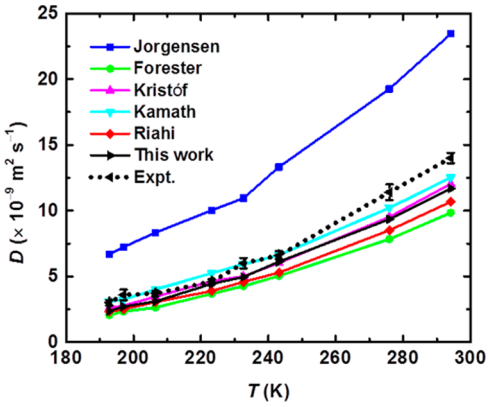

Figure 9. Self-diffusion coefficient of H_2S calculated with the present model and with models from the literature[14−17,21] in the temperature range 192.8−294.1 K, along the experimental liquid−vapor coexistence curve. Experimental values (with error bars) are from ref 11.

calculated and experimental[11] values (see also Table S3, SI). Results are consistent with those reported by Riahi and Rowley.[21] The Jorgensen model overestimates the diffusivity of H_2S over the entire temperature range (likely due to low density), while the Forester model underestimates it. The best agreement with experiment corresponds to the Kamath et al. model.[17] Results from the present Drude model and from the model of Kristóf and Liszi[16] are comparable and in good agreement with experiment. While self-diffusion coefficients from both Drude models (this work and that of Riahi and Rowley[21]) are comparable at low temperature, the present model remains closer to experimental data at high temperatures.

3.7. Hydration of H_2S. Using the regular Lorentz−Berthelot mixing rules, the Drude models of H_2S and H_2O yield a hydration free energy (ΔG_{hyd}) of H_2S of −0.1 ± 0.1 kcal/mol at 298.15 K and 0.1013 MPa (1 atm), in poor agreement with the experimental value (−0.54 kcal/mol).[50,51] In comparison, using the regular Lorentz−Berthelot mixing rules, the Drude model of Riahi and Rowley[21] gives a hydration free energy of 0.24 kcal/mol.[52] To better reproduce the experimental value, pair-specific LJ parameters are optimized between the sulfur atom of H_2S and the oxygen atom of H_2O (see Table 7). These parameters yield ΔG_{hyd} = −0.5 ± 0.1 kcal/mol.

The hydration structure of H_2S is investigated from the simulation of one hydrogen sulfide molecule in 500 water molecules at 298.15 K and 0.1013 MPa. The $g_{SO}(r)$, $g_{SH}(r)$, $g_{HO}(r)$, and $g_{HH}(r)$ RDFs between the hydrogen sulfide solute and its water solvent are reported in Figure 10. For comparison,

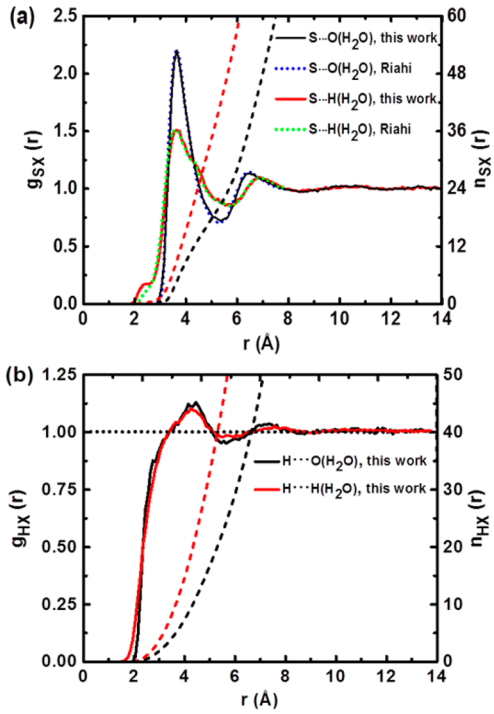

Figure 10. Radial distribution functions, $g(r)$, between a single hydrogen sulfide molecule solvated by 500 water molecules at T = 298.15 K and p = 0.1013 MPa = 1 atm. Panel a shows sulfur−oxygen (black) and sulfur−hydrogen (red) RDFs. Panel b shows hydrogen−oxygen (black) and hydrogen−hydrogen (red) RDFs. Dashed lines represent running coordination numbers, $n(r)$. The green and blue dotted curves in panel a are sulfur−oxygen (blue) and sulfur−hydrogen (green) RDFs produced from ref 52.

we also report the $g_{SO}(r)$ and $g_{SH}(r)$ functions calculated by Riahi and Rowley, who have also calibrated their model to reproduce the hydration free energy of H_2S at 298 K.[52] Remarkably, the $g_{SO}(r)$ function calculated with the present model is almost identical to that from Riahi and Rowley model.[52] It exhibits a first peak with a maximum at 3.64 Å and a minimum at 5.35 Å. Integration up to this minimum shows 20.5 water molecules in the first solvation shell of H_2S, comparable to what is found around an isolated NH_3 (~23 water molecules[20]) and markedly more than around H_2O (4.6 water molecules[18]). The $g_{SH}(r)$ function shows a small shoulder at ~2.4 Å that corresponds to S···H−O hydrogen-bonded pairs. Integration up to the shallow minimum at 2.6 Å yields a coordination number of 0.5. The function also shows a broad peak centered at 3.65 Å with a minimum at ~5.7 Å. Except for the shoulder at ~2.4 Å, the $g_{SH}(r)$ function is in close agreement with that from the Drude model of Riahi and Rowley.[52] The current model shows a higher intensity of the shoulder at ~2.4 Å, in agreement with ab initio MD simulation results.[52] Taking in consideration that both simulations use the same water model, this suggests that the details of the H_2S model have a minimal influence on the hydration structure. Both $g_{HO}(r)$ and $g_{HH}(r)$ RDFs (Figure 10b) show a peak with a maximum at 4.25 Å and a minimum at ~5.7 Å. The absence of a clear peak in the distance range 2−3 Å of $g_{HO}(r)$ indicates that O···H−S hydrogen bonds are weak and transient. Moreover, functions $g_{HO}(r)$ and $g_{HH}(r)$ have the same overall shape, which indicates that the water molecules around the H_2S solute have no significant directionality.

dx.doi.org/10.1021/ct5002335 | J. Chem. Theory Comput. 2014, 10, 3221−3235

The RDFs are consistent with a picture of H_2S hydration in which the molecule is solvated by 20.5 water molecules with minimal hydrogen bonding between solute and solvent molecules.

3.8. Water Solvated in H_2S. Figure 11 reports the $g_{OS}(r)$, $g_{OH}(r)$, $g_{HS}(r)$, and $g_{HH}(r)$. RDFs obtained from the simulation

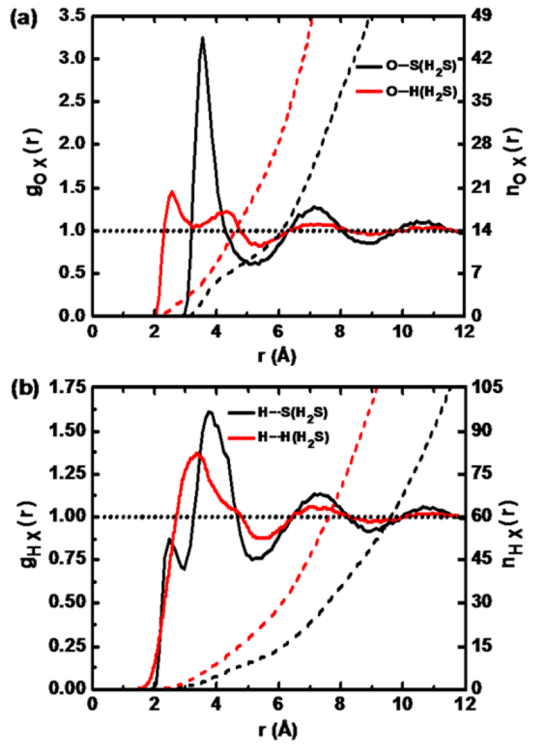

Figure 11. Radial distribution functions, $g(r)$, between a single water molecule solvated by 500 hydrogen sulfide molecules at T = 212.82 K and p = 0.1013 MPa = 1 atm. Panel a shows oxygen–sulfur (black) and oxygen–hydrogen (red) RDFs and panel b shows hydrogen–sulfur (black) and hydrogen–hydrogen (red) RDFs. Dashed lines represent the corresponding running coordination numbers, $n(r)$.

of one water molecule in 500 hydrogen sulfide molecules at 212.82 K and 0.1013 MPa. The $g_{OS}(r)$ function exhibits a first peak at 3.55 Å and a second peak at 7.18 Å. Integration up to the first minimum (at 5.24 Å) shows 9 H_2S molecules in the first solvation shell of H_2O and integration up to the second minimum (at 8.9 Å) shows 48 H_2S molecules in the first and second solvation shells combined. The $g_{OH}(r)$ function exhibits a first peak at 2.55 Å (corresponding to O···H–S hydrogen-bonded pairs) and a second peak at 4.33 Å. Integration up to the first minimum (at 3.25 Å) shows an average of 4.0 hydrogen atoms coordinating the H_2O molecule, most certainly not all forming O···H–S hydrogen bonds. Integration up to the second minimum (at 5.40 Å) gives 21.5 hydrogen atoms, consistent with the ∼10 H_2S molecules in the first solvation shell. The $g_{HS}(r)$ function shows a peak at 2.45 Å corresponding to O–H···S hydrogen-bonded pairs. Integration up to the minimum at 2.96 Å yields a coordination number of 0.9, which suggests that O–H···S contacts are less frequent than O···H–S contacts. Since the force field underestimates the stability of H_2O–H_2S dimer structure 2**a** (forming an O···H–S bond) relative to that of 2**b** (forming an O–H···S bond) (see Figure 2 and Table 2), this preference for O···H–S contacts can be expected to be even greater than what the simulation suggests.

3.9. Solvation of Alkali Ions in H_2S. The model is used to explore the solvation of alkali ions in liquid H_2S. Table 10 shows the calculated absolute solvation free energies of the different alkali ions in liquid H_2S at T = 298.25 K and p = 2.0174 MPa = 19.91 atm. For comparison, the solvation free energies of the alkali ions in liquid water (at T = 298.15 K and p = 0.1013 MPa = 1 atm[26]) and in liquid ammonia (at T = 298.15 K and p = 1.0031 MPa = 9.9 atm)[24] are also reported in Table 10. To the best of our knowledge, no experimental data are available for the solvation thermodynamics of alkali ions in H_2S. Table 10 shows that, while solvation free energies in water and ammonia are comparable,[24] those in hydrogen sulfide are much lower (in absolute value). It is noted, however, that the difference between the solvation free energy of a given ion in water and in hydrogen sulfide decreases on going from Li^+ to Cs^+; it is 33.4 kcal/mol for Li^+, 20.9 kcal/mol for Na^+, 13.5 kcal/mol for K^+, 11.4 kcal/mol for Rb^+, and 6.5 kcal/mol for Cs^+. This reflects the fact that the ion gets softer on going from the smaller Li^+ to the larger Cs^+ and thus its affinity to the hard water relative to the soft hydrogen sulfide decreases.

Table 10. Calculated Absolute (ΔG^{intr}_{solv}) Solvation Free Energies of Alkali Ions in Liquid Water (at T = 298.15 K and p = 0.1013 MPa), Liquid Ammonia (at T = 298.15 K and p = 1.0031 MPa), and Liquid Hydrogen Sulfide (at T = 298.15 K and p = 2.0174 MPa)[a]

	solvent		
ion	H_2O[b]	NH_3[c]	H_2S[d]
Li^+	−109.8	−109.5	−76.4
Na^+	−85.6	−85.0	−64.7
K^+	−67.9	−68.5	−54.4
Rb^+	−63.0	−61.2	−51.6
Cs^+	−55.8	−55.4	−49.3

[a]All values are in kcal/mol. [b]Ref 26. [c]Ref 24. [d]This work.

The structure of alkali ions in liquid H_2S is investigated from MD simulations of each alkali ion in 500 H_2S molecules at 212.82 K and 0.1013 MPa for 10 ns. The structure of H_2S molecules around each ion is analyzed from the distribution functions $g_{ion-S}(r)$ and $g_{ion-H}(r)$. The functions are calculated from the last 8 ns of each MD simulation, and shown in Figure 12. Their characteristics are summarized in Table 11.

The first peak of the $g_{ion-S}(r)$ function decreases in amplitude and shifts away from the ion on going from Li^+ to Cs^+. The coordination number up to the minimum following the first peak is 4.5 for Li^+, 6.0 for Na^+, 8.3 for K^+, 9.6 for Rb^+, and 11.0 for Cs^+ (see Table 11). By comparison, alkali ions in SWM4-NDP water at 212.82 K and 0.1013 MPa display coordination numbers of 4.0 for Li^+, 5.7 for Na^+, 6.6 for K^+, 8.0 for Rb^+, and 9.9 for Cs^+. These numbers are obtained from MD simulations of one alkali ion in 500 water molecules, by integrating the $g_{ion-O}(r)$ function up to its first minimum (at 2.55 Å for Li^+, 3.05 Å for Na^+, 3.35 Å for K^+, 3.65 Å for Rb^+, and 4.05 Å for Cs^+). This is showing that, in its first solvation shell, each alkali ion is surrounded by a larger number of hydrogen sulfide molecules compared to water molecules. While the molecular volume of H_2S is larger than that of H_2O, the observed higher coordination number might be attributed to the larger intermolecular separation between the ions and H_2S. To our

dx.doi.org/10.1021/ct5002335 | J. Chem. Theory Comput. 2014, 10, 3221−3235

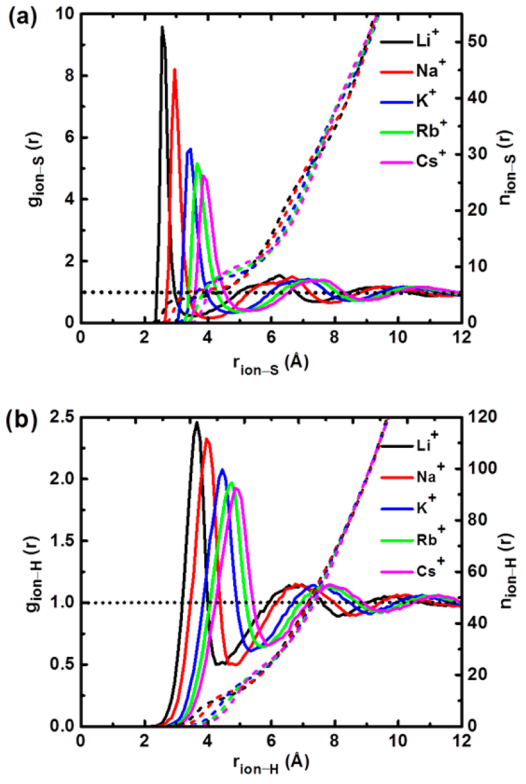

Figure 12. Ion−S (a) and ion−H (b) radial distribution functions (solid curves) and running integration numbers (dashed lines) from molecular dynamics simulations of Li^+ (black), Na^+ (red), K^+ (blue), Rb^+ (green), or Cs^+ (pink) in 500 H_2S molecules at 212.82 K and 0.1013 MPa.

knowledge, no experimental data are available for the solvation structure of alkali ions in H_2S.

3.10. Preferential Solvation of Alkali Ions in Aqueous H_2S. The preferential solvation of the alkali ions in aqueous H_2S is investigated from 85 ns long simulations of each ion in aqueous H_2S solution at molar fraction x_{H_2S} = 0.1 (450 H_2O molecules and 50 H_2S molecules), at T = 212.82 K and p = 0.1013 MPa. We simulate a dilute H_2S mixture because of the low solubility of H_2S in water[38] and to avoid phase separation. Simulations show that the number of H_2S/H_2O molecules in the first solvation shell is 0.00/4.0 for Li^+, 0.02/5.4 for Na^+, 0.02/6.4 for K^+, 0.02/7.4 for Rb^+, and 0.08/7.8 for Cs^+. For the second solvation shell, the number of H_2S/H_2O molecules is 1.4/14.4 for Li^+, 1.7/15.9 for Na^+, 2.1/17.1 for K^+, 2.3/18.5 for Rb^+, and 2.4/18.1 for Cs^+. These coordination numbers are calculated by integrating $g_{ion-S}(r)$ and $g_{ion-O}(r)$ up to the minimum following the first (or second) peak of $g_{ion-(S+O)}(r)$, the total RDF. (The first minimum of $g_{ion-(S+O)}(r)$ is at 2.55 Å for Li^+, 3.05 Å for Na^+, 3.35 Å for K^+, 3.55 Å for Rb^+, and 3.75 Å for Cs^+; the second minimum is at 5.05 Å for Li^+, 5.35 Å for Na^+, 5.65 Å for K^+, 5.75 Å for Rb^+, and 5.95 for Cs^+). These coordination numbers indicate that H_2S molecules are almost totally expelled from the first shell of all ions except Cs^+, whose first shell shows very low occupancy by H_2S. The numbers of H_2S and H_2O molecules in the second shell of each ion are close to their bulk distributions at x_{H_2S} = 0.1 and indicate that the second solvation shells possess no marked selectivity to either ligands.

The results provide insight on the influence of salts on the solubility of H_2S in water. For instance, experiments show that NaCl causes a so-called "salting out" of H_2S, that is, decreases its solubility in water.[53] Based on the binding selectivity of the ions toward water molecules, we suggest that this salting-out effect results from the expulsion of H_2S molecules from the first hydration shells of the ions. This decreases the volume of solution available to H_2S and leads to aggregation and, ultimately, to phase separation. Although not considered in the present work, anions are expected to have a similar selectivity toward water and to further increase the salting-out effect.

4. CONCLUSION

A polarizable potential model for hydrogen sulfide is optimized based on the experimental properties of the H_2S monomer and the density of hydrogen sulfide. The model gives binding energies for hydrogen sulfide clusters in very good agreement with ab initio results. It also yields density, self-diffusion coefficient, and dielectric constant of the liquid at the boiling point in agreement with experiments. Compared to previous models from the literature, the model is showing the best agreement with the experimental structure of liquid H_2S. It is also the most accurate at reproducing the experimental density in the liquid and supercritical phases. It yields self-diffusion coefficient for H_2S in the temperature range 193−294 of the liquid−vapor coexistence curve in good agreement with experiment. The model underestimates the experimental vaporization enthalpy in the temperature range 193−313 of the coexistence curve. This underestimation is however systematic (by ∼0.5 kcal/mol), which allows for a simple post-correction.

The model is calibrated to reproduce the hydration free energy of H_2S, by adjusting pair-specific LJ parameters between S and O, and used to investigate the solvation structure of a single H_2S molecule in liquid H_2O and of a single H_2O molecule in liquid H_2S. Simulations show weak hydrogen

Table 11. Characteristics of the Radial Distribution Functions, $g_{ion-S}(r)$ and $g_{ion-H}(r)$, for a Single Ion in Liquid Hydrogen Sulfide at T = 212.82 K and p = 0.1013 MPa[a]

	$g_{ion-S}(r)$						$g_{ion-H}(r)$					
ion	r_{M1}	r_{m1}	$n(r_{m1})$	r_{M2}	r_{m2}	$n(r_{m2})$	r_{M1}	r_{m1}	$n(r_{m1})$	r_{M2}	r_{m2}	$n(r_{m2})$
Li^+	2.55	3.56	4.5	6.3	7.4	29.0	3.64	4.30	10.3	6.7	8.10	70.4
Na^+	2.95	4.00	6.0	6.7	7.8	34.3	3.96	4.82	14.1	6.8	8.55	82.7
K^+	3.42	4.72	8.3	7.2	8.5	42.4	4.45	5.35	19.0	7.3	9.11	99.9
Rb^+	3.65	4.98	9.6	7.4	8.8	46.7	4.70	5.73	22.9	7.6	9.45	111.4
Cs^+	3.87	5.31	11.0	7.6	9.1	51.2	4.90	5.90	25.0	7.8	9.65	118.7

[a] r_{M1} and r_{M2} are the distances (in Å) where the function has its first and second maximum, respectively. At r_{m1} and r_{m2} (in Å), the function has its first and second minimum. $n(r)$ is the running integration numbers evaluated at $r = r_{m1}$ and r_{m2}.

dx.doi.org/10.1021/ct5002335 | J. Chem. Theory Comput. 2014, 10, 3221−3235

bonding and lower number of hydrogen bonds compared to these between water molecules.

The model is also calibrated to reproduce the ab initio (CCSD(T)) complexation energy of the alkali ion−H_2S pairs, by adjusting pair-specific LJ parameters between S and each alkali ion. While ab initio calculations suggest C_s symmetry for the alkali ion−H_2S pairs, the model gives C_{2v} symmetry. Reproducing the ab initio-observed C_s symmetry of the pairs may require explicit description of the lone pairs of S and mimic the tetrahedral electron-pair geometry of H_2S.

The model was used to investigate the solvation structure and solvation free energy of alkali ions in liquid H_2S, and the preferential solvation of alkali ions in aqueous H_2S. Simulations show that the ions are almost totally solvated by water in their first solvation shells. This is giving insight in the salting-out effect of salts on the solubility of H_2S in water; solvation of the ions by water lower the volume of water available to H_2S molecules and thus decreases their solubility.

In combination with models for hydrocarbons, the present model for H_2S can be used to investigate the properties of binary and complex mixtures between hydrocarbons and H_2S. Such investigations are useful to devise possible separation strategies of H_2S-containing oils and natural gases. The model can also be used to investigate the selectivity of ions toward ligands of different hardness and study their coordination geometry and dynamics around the ions.

■ ASSOCIATED CONTENT

Ⓢ Supporting Information

Three tables including density, heat of vaporization, and self-diffusion coefficient calculated with different H_2S models under different thermodynamic conditions. This material is available free of charge via the Internet at http://pubs.acs.org.

■ AUTHOR INFORMATION

Corresponding Author

*Tel.: +1-514-848-2424, ext. 5314. Fax: +1-514-848-2868. Email: guillaume.lamoureux@concordia.ca.

Notes

The authors declare no competing financial interest.

‡On leave from Department of Chemistry, Faculty of Science, Assiut University, Assiut 71516, Egypt.

■ ACKNOWLEDGMENTS

This work was supported by an NSERC Discovery Grant to G.L. and a Garnet Strong Scholarship and a Power Corporation of Canada graduate fellowship to E.A.O. Computational resources were provided by Calcul Québec.

■ REFERENCES

(1) Bagarinao, T. Sulfide as an environmental factor and toxicant: Tolerance and adaptations in aquatic organisms. *Aquatic Toxicol.* **1992**, *24*, 21−62.

(2) Reiffenstein, R. J.; Hulbert, W. C.; Roth, S. H. Toxicology of hydrogen sulfide. *Annu. Rev. Pharmacol. Toxicol.* **1992**, *32*, 109−134.

(3) EPA. *Report to Congress on Hydrogen Sulfide Air Emissions Associated with the Extraction of Oil and Natural Gas*, EPA-453/R-93-045; Environmental Protection Agency: Washington, DC, 1993.

(4) Li, L.; Rose, P.; Moore, P. K. Hydrogen sulfide and cell signaling. *Annu. Rev. Pharmacol. Toxicol.* **2011**, *51*, 169−187.

(5) Soper, A. K.; Bruni, F.; Ricci, M. A. Site−site pair correlation functions of water from 25 to 400 °C: Revised analysis of new and old diffraction data. *J. Chem. Phys.* **1997**, *106*, 247−254.

(6) Santoli, G.; Bruni, F.; Ricci, F. P.; Ricci, M. A.; Soper, A. K. Orientational correlations in liquid hydrogen sulphide. *Mol. Phys.* **1999**, *97*, 777−786.

(7) Clarke, E. C. W.; Glew, D. N. Deuterium and hydrogen sulfides: Vapor pressures, molar volumes, and thermodynamic properties. *Can. J. Chem.* **1970**, *48*, 764−775.

(8) Ihmels, E. C.; Gmehling, J. Densities of toluene, carbon dioxide, carbonyl sulfide, and hydrogen sulfide over a wide temperature and pressure range in the sub- and supercritical state. *Ind. Eng. Chem. Res.* **2001**, *40*, 4470−4477.

(9) Giauque, W. F.; Blue, B. W. Hydrogen sulfide. The heat capacity and vapor pressure of solid and liquid. The heat of vaporization. A comparison of thermodynamic and spectroscopic values of the entropy. *J. Am. Chem. Soc.* **1936**, *58*, 831−837.

(10) Liessmann, G.; Schmidt, W.; Reiffarth, S. *Recommended Thermophysical Data*; Data Compilation of the Saechsische Olefinwerke: Boehlen, Germany, 1995.

(11) Dupré, F.; Piaggesi, D.; Ricci, F. P. Self-diffusion coefficient in H_2S along the coexistence curve. *Phys. Lett. A* **1980**, *80*, 178−180.

(12) Havriliak, S.; Swenson, R. W.; Cole, R. H. Dielectric constants of liquid and solid hydrogen sulfide. *J. Chem. Phys.* **1955**, *23*, 134−135.

(13) Lemmon, E. W.; McLinden, M. O.; Friend, D. G. Thermophysical properties of fluid systems. In *NIST Chemistry WebBook, NIST Standard Reference Database Number 69*; Linstrom, P. J., Mallard, W. G., Eds.; National Institute of Standards and Technology: Gaithersburg, MD, 2013; http://webbook.nist.gov (accessed on May 13, 2014).

(14) Jorgensen, W. L. Intermolecular potential functions and Monte Carlo simulations for liquid sulfur compounds. *J. Chem. Phys.* **1986**, *90*, 6379−6388.

(15) Forester, T. R.; McDonald, I. R.; Klein, M. L. Intermolecular potentials and the properties of liquid and solid hydrogen sulphide. *Chem. Phys.* **1989**, *129*, 225−234.

(16) Kristóf, T.; Liszi, J. Effective intermolecular potential for fluid hydrogen sulfide. *J. Chem. Phys. B* **1997**, *101*, 5480−5483.

(17) Kamath, G.; Lubna, N.; Potoff, J. J. Effect of partial charge parametrization on the fluid phase behavior of hydrogen sulfide. *J. Chem. Phys.* **2005**, *123*, 124505-1−124505-7.

(18) Lamoureux, G.; Harder, E.; Vorobyov, I. V.; Roux, B.; MacKerell, A. D. A polarizable model of water for molecular dynamics simulations of biomolecules. *Chem. Phys. Lett.* **2006**, *418*, 245−249.

(19) Almeida, T. S.; Coutinho, K.; Cabral, B. J. C.; Canuto, S. Electronic properties of liquid ammonia: A sequential molecular dynamics/quantum mechanics approach. *J. Chem. Phys.* **2008**, *128*, 014506-1−014506-9.

(20) Orabi, E. A.; Lamoureux, G. Polarizable interaction model for liquid, supercritical, and aqueous ammonia. *J. Chem. Theory Comput.* **2013**, *9*, 2035−2051.

(21) Riahi, S.; Rowley, C. N. A Drude polarizable model for liquid hydrogen sulfide. *J. Phys. Chem. B* **2013**, *117*, 5222−5229.

(22) Plambeck, J. A. Solvation thermodynamics of ions: Free energies in water, ammonia, and fused LiCI-KC1 eutectic. *Can. J. Chem.* **1969**, *47*, 1401−1410.

(23) Tuttle, T. R.; Malaxos, S.; Coe, J. V. A new cluster pair method of determining absolute single ion solvation energies demonstrated in water and applied to ammonia. *J. Phys. Chem. A* **2002**, *106*, 925−932.

(24) Orabi, E. A.; Lamoureux, G. Molecular dynamics investigation of alkali metal ions in liquid and aqueous ammonia. *J. Chem. Theory Comput.* **2013**, *9*, 2324−2338.

(25) Tissandier, M. D.; Cowen, K. A.; Feng, W. Y.; Gundlach, E.; Cohen, M. H.; Earhart, A. D.; Coe, J. V. The proton's absolute aqueous enthalpy and Gibbs free energy of solvation from cluster−ion solvation data. *J. Phys. Chem. A* **1998**, *102*, 7787−7794.

(26) Yu, H.; Whitfield, T.; Harder, E.; Lamoureux, G.; Vorobyov, I.; Anisimov, V. M.; MacKerell, A. D.; Roux, B. Simulating monovalent and divalent ions in aqueous solution using a Drude polarizable force field. *J. Chem. Theory Comput.* **2010**, *6*, 774−786.

(27) Frisch, M. J.; Trucks, G. W.; Schlegel, H. B.; Scuseria, G. E.; Robb, M. A.; Cheeseman, J. R.; Scalmani, G.; Barone, V.; Mennucci,

B.; Petersson, G. A.; Nakatsuji, H.; Caricato, M.; Li, X.; Hratchian, H. P.; Izmaylov, A. F.; Bloino, J.; Zheng, G.; Sonnenberg, J. L.; Hada, M.; Ehara, M.; Toyota, K.; Fukuda, R.; Hasegawa, J.; Ishida, M.; Nakajima, T.; Honda, Y.; Kitao, O.; Nakai, H.; Vreven, T.; Montgomery, Jr., J. A.; Peralta, J. E.; Ogliaro, F.; Bearpark, M.; Heyd, J. J.; Brothers, E.; Kudin, K. N.; Staroverov, V. N.; Kobayashi, R.; Normand, J.; Raghavachari, K.; Rendell, A.; Burant, J. C.; Iyengar, S. S.; Tomasi, J.; Cossi, M.; Rega, N.; Millam, J. M.; Klene, M.; Knox, J. E.; Cross, J. B.; Bakken, V.; Adamo, C.; Jaramillo, J.; Gomperts, R.; Stratmann, R. E.; Yazyev, O.; Austin, A. J.; Cammi, R.; Pomelli, C.; Ochterski, J. W.; Martin, R. L.; Morokuma, K.; Zakrzewski, V. G.; Voth, G. A.; Salvador, P.; Dannenberg, J. J.; Dapprich, S.; Daniels, A. D.; Farkas, Ö.; Foresman, J. B.; Ortiz, J. V.; Cioslowski, J.; Fox, D. J. *Gaussian 09*, Revision B.01; Gaussian, Inc.: Wallingford, CT, 2009.

(28) (a) Dunning, T. H., Jr. Gaussian basis sets for use in correlated molecular calculations. I. The atoms boron through neon and hydrogen. *J. Chem. Phys.* **1989**, *90*, 1007−1023. (b) Kendall, R. A.; Dunning, T. H., Jr.; Harrison, R. J. Electron affinities of the first-row atoms revisited. Systematic basis sets and wave functions. *J. Chem. Phys.* **1992**, *96*, 6796−6806. (c) Woon, D. E.; Dunning, T. H., Jr. Gaussian basis sets for use in correlated molecular calculations. III. The atoms aluminum through argon. *J. Chem. Phys.* **1993**, *98*, 1358−1371. (d) Woon, D. E.; Dunning, T. H., Jr. Gaussian basis sets for use in correlated molecular calculations. IV. Calculation of static electrical response properties. *J. Chem. Phys.* **1994**, *100*, 2975−2988.

(29) The Stuttgart relativistic small core basis set was obtained from EMSL Basis Set Library at https://bse.pnl.gov/bse/portal (accessed May 13, 2014). For the original valence basis set and ECP reference, see Bergner, A.; Dolg, M.; Kuechle, W.; Stoll, H.; Preuss, H. Ab initio energy-adjusted pseudopotentials for elements of groups 13−17. *Mol. Phys.* **1993**, *80*, 1431−1441.

(30) Boys, S.; Bernardi, F. The calculation of small molecular interactions by the differences of separate total energies. Some procedures with reduced errors. *Mol. Phys.* **1970**, *19*, 553−566.

(31) Brooks, B. R.; Brooks, C. L.; Mackerell, A. D.; Nilsson, L.; Petrella, R. J.; Roux, B.; Won, Y.; Archontis, G.; Bartels, C.; Boresch, S.; Caflisch, A.; Caves, L.; Cui, Q.; Dinner, A. R.; Feig, M.; Fischer, S.; Gao, J.; Hodoscek, M.; Im, W.; Kuczera, K.; Lazaridis, T.; Ma, J.; Ovchinnikov, V.; Paci, E.; Pastor, R. W.; Post, C. B.; Pu, J. Z.; Schaefer, M.; Tidor, B.; Venable, R. M.; Woodcock, H. L.; Wu, X.; Yang, W.; York, D. M.; Karplus, M. CHARMM: The biomolecular simulation program. *J. Comput. Chem.* **2009**, *30*, 1545−1614.

(32) Lamoureux, G.; Roux, B. Modeling induced polarization with classical Drude oscillators: Theory and molecular dynamics simulation algorithm. *J. Chem. Phys.* **2003**, *119*, 3025−3039.

(33) Orabi, E. A.; Lamoureux, G. Cation−π and π−π interactions in aqueous solution studied using polarizable potential models. *J. Chem. Theory Comput.* **2012**, *8*, 182−193.

(34) Lamoureux, G.; Orabi, E. A. Molecular modelling of cation−π interactions. *Mol. Simul.* **2012**, *38*, 704−722.

(35) Wang, S.; Orabi, E. A.; Baday, S.; Bernèche, S.; Lamoureux, G. Ammonium transporters achieve charge transfer by fragmenting their substrate. *J. Am. Chem. Soc.* **2012**, *134*, 10419−10427.

(36) Martyna, G. J.; Tuckerman, M. E.; Tobias, D. J.; Klein, M. L. Explicit reversible integrators for extended systems dynamics. *Mol. Phys.* **1996**, *87*, 1117−1157.

(37) Herzberg, G. *Electronic Spectra and Electronic Structure of Polyatomic Molecules*; Van Nostrand: New York, 1966.

(38) Zezin, D. Yu.; Migdisov, A. A.; Williams-Jones, A. E. PVTx properties of H_2O−H_2S fluid mixtures at elevated temperature and pressure based on new experimental data. *Geochim. Cosmochim. Acta* **2011**, *75*, 5483−5495.

(39) Essmann, U.; Perera, L.; Berkowitz, M. L.; Darden, T.; Lee, H.; Pedersen, L. G. A smooth particle mesh Ewald method. *J. Chem. Phys.* **1995**, *103*, 8577−8593.

(40) Lagüe, P.; Pastor, R. W.; Brooks, B. R. Pressure-based long-range correction for Lennard-Jones interactions in molecular dynamics simulations: Application to alkanes and interfaces. *J. Phys. Chem. B* **2004**, *108*, 363−368.

(41) Hoover, W. G. Canonical dynamics: Equilibrium phase-space distributions. *Phys. Rev. A* **1985**, *31*, 1695−1697.

(42) Martyna, G. J.; Tobias, D. J.; Klein, M. L. Constant pressure molecular dynamics algorithms. *J. Chem. Phys.* **1994**, *101*, 4177−4189.

(43) Yeh, I.-C.; Hummer, G. System-size dependence of diffusion coefficients and viscosities from molecular dynamics simulations with periodic boundary conditions. *J. Phys. Chem. B* **2004**, *108*, 15873−15879.

(44) Neumann, M.; Steinhauser, O. Computer simulation and the dielectric constant of polarizable polar systems. *Chem. Phys. Lett.* **1984**, *106*, 563−569.

(45) Buckingham, A. D. A Theory of the Dielectric Polarization of Polar Substances. *Proc. R. Soc. London, Ser. A* **1956**, *238*, 235−244.

(46) Hoy, A. R.; Bunker, P. R. A precise solution of the rotation bending Schrödinger equation for a triatomic molecule with application to the water molecule. *J. Mol. Spectrosc.* **1979**, *74*, 1−8.

(47) Nelson, R. D.; Lide, D. R.; Maryott, A. A. Selected values of electric dipole moments for molecules in the gas phase. *National Standard Reference Data Series, National Bureau of Standards 10*; NIST, Washington, DC, 1967, http://www.nist.gov/data/nsrds/NSRDS-NBS-10.pdf (accessed on May 13, 2014).

(48) Olney, T. N.; Cann, N. M.; Cooper, G.; Brion, C. E. Absolute scale determination for photoabsorption spectra and the calculation of molecular properties using dipole sum rules. *Chem. Phys.* **1997**, *223*, 59−98.

(49) Shimanouchi, T. Tables of molecular Vibrational frequencies I. *National Standard Reference Data Series National Bureau of Standards 39*; NIST, Washington, DC, 1972, http://www.nist.gov/data/nsrds/NSRDS-NBS-39.pdf (accessed on May 13, 2014).

(50) Wilhelm, E.; Battino, R.; Wilcock, R. J. Low-pressure solubility of gases in liquid water. *Chem. Rev.* **1977**, *77*, 219−262.

(51) Kubo, M. M.; Gallicchio, E.; Levy, R. M. Thermodynamic decomposition of hydration free energies by computer simulation: Application to amines, oxides, and sulfides. *J. Phys. Chem. B* **1997**, *101*, 10527−10534.

(52) Riahi, S.; Rowley, C. N. Solvation of hydrogen sulfide in liquid water and at the water−vapor interface using a polarizable force field. *J. Phys. Chem. B* **2014**, *118*, 1373−1380.

(53) Suleimenov, O. M.; Krupp, R. E. Solubility of hydrogen sulfide in pure water and in NaCl solutions, from 20 to 320 °C and at saturation pressures. *Geochim. Cosmochim. Acta* **1994**, *58*, 2433−2444.